



High-order soliton evolution and pulse breaking-recovery in stretched ultrafast fiber lasers

YUEQING DU, XUEWEN SHU,* HAO ZHANG, AND PEIYUN CHENG

Wuhan National Laboratory for Optoelectronics & School of Optical and Electronic Information,
Huazhong University of Science and Technology, Wuhan, 430074, China

*xshu@hust.edu.cn

Abstract: We present a new pulse regime in a stretched ultrafast fiber laser based on numerical simulations. The pulse breaking due to high-order soliton evolution in the passive fiber is recovered to a smooth pulse in the gain fiber with normal dispersion. The new pulse regime formed by the two nonlinear processes makes the ultrafast fiber laser generate ultra-broadband, ultrashort duration, high energy and large breathing ratio pulses. Our work gives insights into the nonlinear dynamics in fiber lasers and has potential for a better design of the stretched fiber lasers.

© 2018 Optical Society of America under the terms of the [OSA Open Access Publishing Agreement](#)

OCIS codes: (060.5530) Pulse propagation and temporal solitons; (140.4050) Mode-locked lasers; (140.3510) Lasers, fiber.

References and links

1. M. E. Fermann and I. Hartl, "Ultrafast fibre lasers," *Nat. Photonics* **7**(11), 868–875 (2013).
2. L. G. Wright, D. N. Christodoulides, and F. W. Wise, "Spatiotemporal mode-locking in multimode fiber lasers," *Science* **358**(6359), 94–97 (2017).
3. M. Pang, W. He, X. Jiang, and P. St. J. Russell, "All-optical bit storage in a fiber laser by optomechanically bound state of solitons," *Nat. Photonics* **10**(2), 1–6 (2016).
4. V. J. Matsas, D. J. Richardson, T. P. Newson, and D. N. Payne, "Characterization of a self-starting, passively mode-locked fiber ring laser that exploits nonlinear polarization evolution," *Opt. Lett.* **18**(5), 358–360 (1993).
5. L. E. Nelson, D. J. Jones, K. Tamura, H. A. Haus, and E. P. Ippen, "Ultrashort-pulse fiber ring lasers," *Appl. Phys. B* **65**(2), 277–294 (1997).
6. F. W. Wise, A. Chong, and W. H. Renninger, "High-energy femtosecond fiber lasers based on pulse propagation at normal dispersion," *Laser Photonics Rev.* **2**(1–2), 58–73 (2008).
7. K. Tamura, L. E. Nelson, H. A. Haus, and E. P. Ippen, "Soliton versus nonsoliton operation of fiber ring lasers," *Appl. Phys. Lett.* **64**(2), 149–151 (1994).
8. K. Tamura, E. P. Ippen, H. A. Haus, and L. E. Nelson, "77-fs pulse generation from a stretched-pulse mode-locked all-fiber ring laser," *Opt. Lett.* **18**(13), 1080–1082 (1993).
9. H. A. Haus, K. Tamura, L. E. Nelson, and E. P. Ippen, "Stretched-Pulse Additive Pulse Mode-Locking in Fiber Ring Lasers: Theory and Experiment," *IEEE J. Quantum Electron.* **31**(3), 591–598 (1995).
10. F. O. Ilday, F. W. Wise, and T. Sosnowski, "High-energy femtosecond stretched-pulse fiber laser with a nonlinear optical loop mirror," *Opt. Lett.* **27**(17), 1531–1533 (2002).
11. L. Lefort, J. H. V. Price, D. J. Richardson, G. J. Spüler, R. Paschotta, U. Keller, A. R. Fry, and J. Weston, "Practical low-noise stretched-pulse Yb³⁺-doped fiber laser," *Opt. Lett.* **27**(5), 291–293 (2002).
12. A. Wienke, F. Haxsen, D. Wandt, U. Morgner, J. Neumann, and D. Kracht, "Ultrafast, stretched-pulse thulium-doped fiber laser with a fiber-based dispersion management," *Opt. Lett.* **37**(13), 2466–2468 (2012).
13. J. Sotor, I. Pasternak, A. Krajewska, W. Strupinski, and G. Sobon, "Sub-90 fs stretched-pulse mode-locked fiber laser based on a graphene saturable absorber," *Opt. Express* **23**(21), 27503–27508 (2015).
14. D. A. Dvoretzkiy, V. A. Lazarev, V. S. Voropaev, Z. N. Rodnova, S. G. Sazonkin, S. O. Leonov, A. B. Pnev, V. E. Karasik, and A. A. Krylov, "High-energy, sub-100 fs, all-fiber stretched-pulse mode-locked Er-doped ring laser with a highly-nonlinear resonator," *Opt. Express* **23**(26), 33295–33300 (2015).
15. P. Grelu and N. Akhmediev, "Dissipative solitons for mode-locked lasers," *Nat. Photonics* **6**(2), 84–92 (2012).
16. L. M. Zhao, D. Y. Tang, and J. Wu, "Gain-guided soliton in a positive group-dispersion fiber laser," *Opt. Lett.* **31**(12), 1788–1790 (2006).
17. D. Ma, Y. Cai, C. Zhou, W. Zong, L. Chen, and Z. Zhang, "37.4 fs pulse generation in an Er:fiber laser at a 225 MHz repetition rate," *Opt. Lett.* **35**(17), 2858–2860 (2010).
18. L. M. Zhao, D. Y. Tang, T. H. Cheng, and C. Lu, "Ultrashort pulse generation in lasers by nonlinear pulse amplification and compression," *Appl. Phys. Lett.* **90**(5), 051102 (2007).

19. L. M. Zhao, D. Y. Tang, H. Y. Tam, and C. Lu, "Pulse breaking recovery in fiber lasers," *Opt. Express* **16**(16), 12102–12107 (2008).
20. S. Chouli, J. M. Soto-Crespo, and P. Grelu, "Optical spectra beyond the amplifier bandwidth limitation in dispersion-managed mode-locked fiber lasers," *Opt. Express* **19**(4), 2959–2964 (2011).
21. L. F. Mollenauer, R. H. Stolen, and J. P. Gordon, "Experimental Observation of Picosecond Pulse Narrowing and Solitons in Optical Fibers," *Phys. Rev. Lett.* **45**(13), 1095–1098 (1980).
22. K. A. Ahmed, K. C. Chan, and H. F. Liu, "Femtosecond Pulse Generation from Semiconductor Lasers Using the Soliton-Effect Compression Technique," *IEEE J. Sel. Top. Quantum Electron.* **1**(2), 592–600 (1995).
23. R. H. Stolen, L. F. Mollenauer, and W. J. Tomlinson, "Observation of pulse restoration at the soliton period in optical fibers," *Opt. Lett.* **8**(3), 186–188 (1983).
24. S. A. Planas, N. L. P. Mansur, C. H. B. Cruz, and H. L. Fragnito, "Spectral narrowing in the propagation of chirped pulses in single-mode fibers," *Opt. Lett.* **18**(9), 699–701 (1993).
25. H. Luo, L. Zhan, L. Zhang, Z. Q. Wang, C. X. Gao, and X. Fang, "Generation of 22.7-fs 2.8-nJ Pulse From an Erbium-Doped All-Fiber Laser via Single Stage Soliton Compression," *J. Lightwave Technol.* **35**(17), 3780–3784 (2017).
26. H. Luo, L. Zhan, Z. Q. Wang, L. Zhang, C. Feng, and X. H. Shen, "All-Fiber Generation of Sub-30 fs Pulses at 1.3- μ m via Cherenkov Radiation with Entire Dispersion Management," *J. Lightwave Technol.* **35**(11), 2325–2330 (2017).

1. Introduction

Ultrafast fiber lasers have attracted lots of research interests due to their compact structures, cost-effective design and excellent pulse properties [1–3]. Ultrafast fiber lasers at anomalous-dispersion generate the soliton-like pulse, whose energy is limited to ~ 100 pJ due to the soliton-area theorem [4–7]. Pulse-breaking happens due to the over-driving of the nonlinear phase accumulation when the soliton has large pulse energy. Researchers proposed using dispersion management to make the pulse stretch and compress in the near zero-dispersion cavity [8, 9], which can reduce the average pulse intensity as well as the nonlinear phase accumulation. Usually, the pulse energy output from a stretched fiber laser ranges from ~ 100 pJ to ~ 3 nJ [10–14] and generating higher pulse energy needs normal-dispersion [15, 16] to obtain dissipative solitons or gain-guided solitons (GGs). In the stretched fiber lasers, dispersion management dominates the pulse dynamics rather than the nonlinear processes. Researchers tend to reduce the nonlinearity for high energy pulse generation, which might sacrifice the bandwidth and duration of the ultrashort pulse. The bandwidth directly output from stretched fiber lasers is usually ~ 50 nm, which corresponds to a transform-limited pulse duration of ~ 100 fs [10–14]. To obtain transform-limited pulse with ultra-broadband spectrum has potential in optical fiber communications and optical sampling. The nonlinear pulse shaping has been employed in the GGS and stretched fiber lasers to generation pulses with ultra-broadband spectrum and ultrashort duration [17–19]. For example, researchers obtained an ultrashort pulse with 135 nm directly from a stretched fiber laser, which was compressed to 37.4 fs with prism pairs [17]. Through nonlinear pulse compression, an ultrashort pulse with 56 fs duration and a 53 nm bandwidth has been obtained directly from a GGS fiber laser [18]. It was proposed in [19] that the gain fiber with normal dispersion can recover the broken pulse in the passive fiber with anomalous-dispersion to a smooth pulse, which is called the pulse-breaking recovery (PBR). Spectral breathing effect in a stretched fiber laser [20] has potential in broadband pulse generation beyond the gain bandwidth limitation. The above works on the nonlinear properties of the stretched fiber lasers illustrate that the nonlinearity is not always harmful while sometimes helpful for the stretched fiber lasers, however, literatures still lack the research on the nonlinear characteristics of the stretched fiber lasers. A recent work on single stage soliton compression shows that the external high-order soliton (HOS) evolution can be used to generate few-cycle pulses [25] with high energy and broadband spectrum beyond the gain bandwidth, what's more, the external pulse evolution in [25] behaves like a stretched pulse in a fiber laser, which inspires us to research whether the similar nonlinear evolution can happen in the stretched ultrafast fiber lasers. It has also been shown in [26] that through the external HOS fission and Cherenkov Radiation, the mode-locked pulse can be compressed to a sub-30 fs pulse. One can get from [25, 26] that the HOS can be used to generate the transform-limited pulse with ultra-narrow width and broadband spectrum. It is curious for us to know whether the

nonlinearity in the fiber laser can be used to directly generate ultra-narrow pulse from the cavity.

In this paper, we present a new working regime for the stretched fiber lasers based on numerical simulations, which can generate ultrashort pulses with ultra-broadband spectrum directly without external compression. Two nonlinear processes are used in the new regime, one is the high-order soliton (HOS) evolution in the passive fiber with anomalous-dispersion, the other is the PBR in the gain fiber with normal-dispersion. The pulse compression of HOS results in ultrashort and ultra-broadband pulse generation, however, pulse breaking happens due to the HOS evolution [21–23], which is compensated by the PBR in the gain fiber. The normal-dispersion of the gain fiber plays an essential role in the PBR because it compensates the nonlinear chirp of the broken pulse. The HOS evolution together with the PBR ensures the nonlinear stretched-pulse evolves with cavity boundary conditions satisfied. Our work gives insights into the nonlinear dynamics of ultrafast fiber lasers and is useful for stretched fiber laser design.

2. Model and parameters in simulations

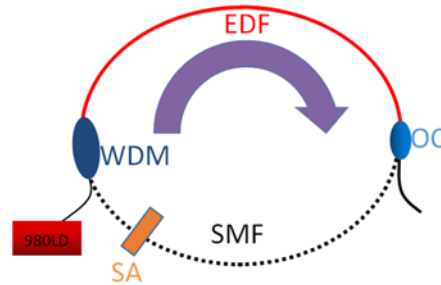


Fig. 1. Schematic of the fiber laser in our simulation. LD:laser diode, WDM:wavelength division multiplexer, OC: output coupler, SA: saturable absorber, EDF: Er-doped fiber, SMF: single mode fiber.

The fiber laser model that we use in our simulation is schematically shown in Fig. 1. The cavity includes a 2m Er-doped fiber (EDF), a segment of single-mode fiber (SMF), a saturable absorber (SA) and an output coupler (OC). The OC has an output ratio of 10:90. Our simulation runs from the EDF to the SMF in each round as shown in Fig. 1. We use the complex Ginzburg-Landau equation (CGLE) to describe the pulse propagating in the laser cavity:

$$\frac{\partial u}{\partial z} = -\frac{1}{2}i\beta_2 \frac{\partial^2 u}{\partial T^2} + \frac{1}{6}i\beta_3 \frac{\partial^3 u}{\partial T^3} + i\gamma|u|^2 u + \frac{1}{2}g \left(1 + \frac{1}{\Omega^2} \frac{\partial^2}{\partial T^2} \right) u \quad (1)$$

Where u represents the slow varying envelop of the optical field and T is the retarded time. β_2 is the second-order dispersion, which is $50\text{ps}^2/\text{km}$ in EDF and $-23\text{ps}^2/\text{km}$ in SMF. β_3 is the third-order dispersion (TOD), which is $0.1\text{ps}^3/\text{km}$. γ is the nonlinearity of the fiber, which is $4.7\text{W}^{-1}\text{km}^{-1}$ and $1.3\text{W}^{-1}\text{km}^{-1}$ in EDF and SMF, respectively. Ω represents the gain bandwidth of the EDF and the full width of half maximum (FWHM) of the gain bandwidth is 20nm in our simulation. g is the gain of the EDF, which is represented by:

$$g = g_0 \exp\left(-\int |u|^2 dt / Es\right) \quad (2)$$

Where Es is the saturable energy of the gain fiber, which represents the pump strength. g_0 is the small signal gain of the EDF, which is 2.5m^{-1} . The transmission function of the amplitude of the lumped SA is represented by:

$$T = \sqrt{1 - \alpha / (1 + P / P_0)} \quad (3)$$

Where α is the modulation depth of the SA, which is 0.7 in our simulation. The high modulation depth of the SA is to suppress the dispersion-gap in dispersion-managed fiber laser, where the laser is unstable due to the unfiltered continuous-wave. P_0 is the saturation power of the SA, which is 100W in our simulation. The parameters are chosen to make the simulation converge quickly. For simplicity, we use the monotonic model and the parameters of the SA have no obvious effects on the main conclusions of this paper. We vary the length of SMF to adjust the net-dispersion of the laser cavity in the simulations. We use the symmetric split-step Fourier method to implement our simulations. We run the programs for 10000 rounds for each case in our simulations.

Due to the TOD effect, the pulse profile and its spectrum are not symmetric in both temporal and spectral domains, so we use the average width to describe the pulse widths in temporal and frequency domains:

$$\sigma_t = \sqrt{\frac{\int T^2 |u|^2 dT}{\int |u|^2 dT} - \left[\frac{\int T |u|^2 dT}{\int |u|^2 dT} \right]^2} \quad (4)$$

$$\sigma_f = \sqrt{\frac{\int f^2 |F_u|^2 df}{\int |F_u|^2 df} - \left[\frac{\int f |F_u|^2 df}{\int |F_u|^2 df} \right]^2} \quad (5)$$

Where T is the retarded time, u is the amplitude of the pulse and σ_t is the average temporal width. f , F_u and σ_f are frequency offset from the central frequency, Fourier transformation of u and average frequency width, respectively.

3. Results

3.1 quasi-linear stretched-pulse evolution

A stretched-pulse that experiences slightly nonlinear effect can be regarded as a quasi-linear wave in the laser cavity, whose dynamics are dominated by the linear dispersion management while nonlinearity is weak due to the reduced average intensity. We set the net-dispersion to be zero, which corresponds to a cavity length of 6.35m, and the pump strength to be 120pJ. The typical stretched-pulse is shown in Fig. 2. One can get from Fig. 2(a) that the pulse breathes twice in one round, which is the typical stretched-pulse behavior [9]. We can obtain from Fig. 2(b) that the spectrum experiences narrowing at the beginning of the gain fiber, which is caused by the gain filtering [16] and spectral narrowing of chirped pulse at normal-dispersion [24]. There are slight spectral broadening at ~4m, which is due to the strong self-phase modulation (SPM) of the narrow pulse with strong intensity. Figure 2(c) shows the evolutions of the average temporal and frequency width of the stretched pulse. We can get from Fig. 2(c) that the breathing ratio of the average temporal and spectral width in the cavity are 5.06 and 3.04, respectively. Except at some specific positions in the cavity (0.76-1.69m, 3.89-4.46m), there is no obvious nonlinear spectral broadening and thus such a stretched-pulse in Fig. 2 can be regarded as a quasi-linear wave. The minimum FWHM in temporal and and maximum FWHM in spectral domains are 117fs and 53nm, respectively, which are typical values of the stretched-pulse. One can see from Fig. 2(d) that the pulse has a typical Gaussian profile at the end of the EDF while some fine structures emerge when the pulse is at the end of the cavity. We can get from Fig. 2(d) that the pulse at the end of EDF has FWHM of 1.12ps and peak power of 279W, which corresponds to a 2.5-order soliton with positive chirp. It is known that the soliton with order larger than 2 will experience pulse breaking during its evolution while no fine structures can be observed if the soliton order is smaller than 2 [23]. The pulse energy inside the cavity ranges from 178pJ to 249pJ. We find that there are no fine structures when the pump strength is below 100pJ, where the soliton order of the pulse at the end of the EDF is below ~2.1, so it is suitable for us to speculate that the fine structures in Fig. 2 are related to a HOS evolution.

There is no doubt that the distorted pulse at the end of the cavity is caused by the nonlinear effect, which inspires us to further research the physical picture of the stretched-pulse with stronger nonlinearity.

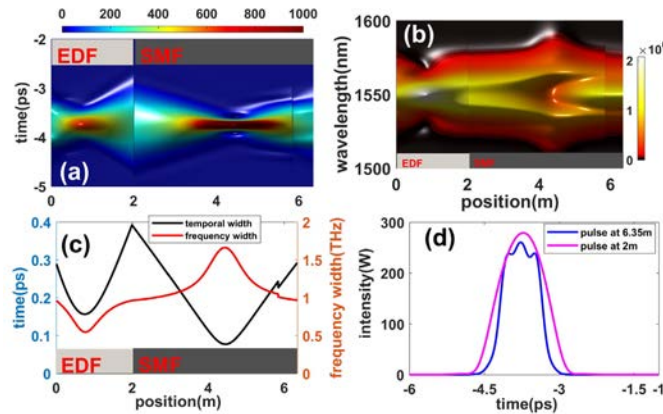


Fig. 2. Intra-cavity pulse characteristics with 120pJ pump strength, near-zero net-dispersion: (a) pulse evolution in temporal domain, (b) pulse evolution in spectral domain, (c) average temporal and frequency width evolution, (d) intensity profiles at two positions.

3.2 nonlinear stretched-pulse evolution

With the pump strength increasing while keeping the other parameters fixed, we can obtain pulse breaking and recovery behaviors when the pump strength is larger than 150pJ. We set the pump strength to be 1300pJ and the results are shown in Fig. 3. Considering the dramatic amplitude change in the cavity and in order to show clear intra-cavity evolution of the stretched-pulse, we plot the normalized pulse profiles and spectra at each locations in the cavity, which are shown in Figs. 3(a) and 3(b), respectively. We can see from Fig. 3(a) that the structured pulse in the EDF gradually self-organizes into a smooth profile at ~ 1.2 m. The smooth pulse experiences broadening and narrowing as the stretched-pulse with weak nonlinearity. After the pulse is compressed to its minimum duration at 3.71m, the pulse splits step-by-step as shown in Fig. 3(a). Such pulse compressing and splitting behaviors remind us of the HOS evolution in anomalous-dispersion fibers [21]. One can see from Fig. 3(b) that the self-organized structure at the beginning of the EDF also happens in spectral domain, which is caused by the gain-filtering and chirped-pulse spectral narrowing [16, 24]. After the spectral narrowing in EDF, the spectrum broadens and multi-peaks emerge on the spectrum due to the SPM. Strong spectral broadening happens at ~ 3.44 – ~ 4.34 m, which is accompanied by the pulse narrowing as shown in Fig. 3(a). We can obtain from Fig. 3(b) that the spectra of the pulse are much more structured and broad than the smooth spectrum of the linear stretched-pulse in Fig. 2(b). We can get from Fig. 3(c) that the nonlinear stretched-pulse also stretches and compresses twice in one round as the linear stretched-pulse doing. The spectral width in Fig. 3(d) experiences a strong nonlinear oscillation at ~ 3.44 – ~ 4.34 m. The average temporal and spectral breathing ratio are 3.09 and 8.1, respectively. We should note that the average temporal and spectral width for the structured and asymmetric pulse in Figs. 3(a) and 3(b) describe the effective distribution of the pulse in temporal and spectral domains, which have strong deviation from the FWHM of the pulse. For example, the FWHM of the central peak of the pulse at 3.71m is 39.1fs while its average width calculated by Eq. (5) is 247fs. The temporal breathing ratio of the FWHM is ~ 51 , which is one order magnitude higher than that of the average temporal breathing ratio of 3.09. The pulse intensity profiles and spectra at several positions in the cavity are shown in Figs. 3(e) and 3(f), respectively. We can see from Fig. 3(e) that the pulse at the end of EDF has a smooth profile with FWHM of 1.99ps and peak power of 1.57kW, which means the pulse has a soliton order of ~ 10.6 assuming it has a sech² profile. After propagation in the SMF for ~ 1.71 m, the pulse is

compressed to an ultra-narrow pulse with 39.1fs FWHM and 33kW peak power. The pulse at 3.71m has pedestals at both sides, which is a typical characteristic in the HOS evolution [21]. The pulse splits into two asymmetric peaks at 4.05m due to TOD. The pulse at 6.35m is more broadened with several peaks due to the HOS evolution. The fine structures and peaks of the spectra in Fig. 3(f) are caused by the strong nonlinear phase accumulation. The pulse at 4.05m has average spectral width of 55.6nm and FWHM of 129nm, which is far beyond the 20nm gain bandwidth. The pulse energy inside the cavity ranges from 2.3nJ to 2.9nJ, which is an order of magnitude higher than that of the linear stretched-pulse. [Visualization 1](#) shows the pulse evolution inside the laser cavity in the case of Fig. 3. We can see from the [Visualization 1](#) that the pulse evolution in the SMF is a typical HOS evolution, even there are some differences with the strict HOS evolution with soliton order of 10.6, which will be discussed in the following paragraph.

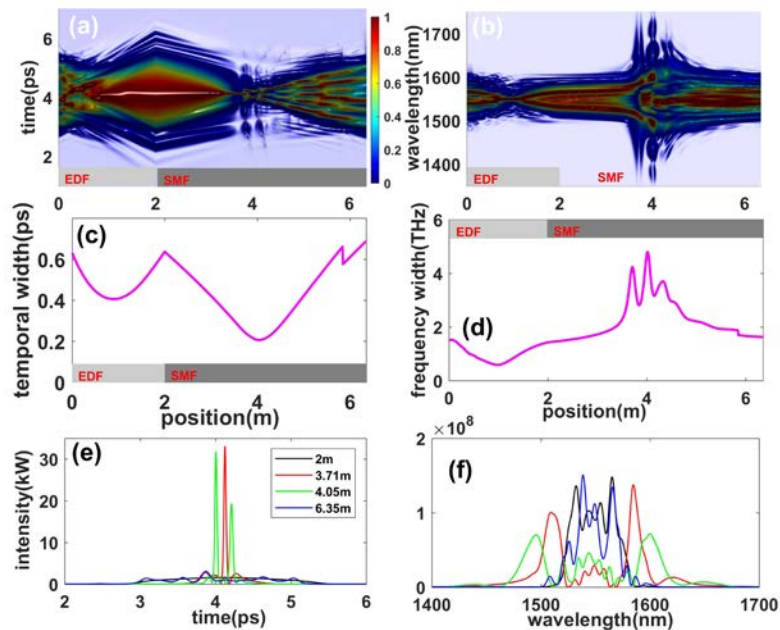


Fig. 3. Pulse characteristics with 1300pJ pump strength, 70% modulation depth and near-zero net-dispersion: (a) pulse evolution in temporal domain, (b) pulse evolution in spectral domain, (c) pulse energy evolution, (d) evolution of frequency width of the soliton, (e) pulse intensity profiles at different locations, (f) pulse spectra at different locations.

We continue increasing the pump strength until pulse splitting to investigate the pulse dynamics. The minimum FWHM of stretched-pulse and its optimal compression distance (position where the HOS is compressed to the minimum width in the SMF for the first time) under different pump strengths are shown in Fig. 4(a). We can get from Fig. 4(a) that the minimum width inside the cavity gradually decreases as the pump strength increasing and finally saturates to ~ 40 fs when the pump strength reaches ~ 600 pJ. We find that the minimum FWHM at the saturated pump strength depends on the net-dispersion, for example, the minimum FWHMs for the net-dispersion of -0.01ps^2 and 0.01ps^2 are 29fs and 44fs, respectively. The HOS evolution in the cavity is not exactly the same as its propagation in a segment of SMF because its evolution should be adapted to the boundary conditions and cavity parameters. What's more, the pulse at the end of EDF is positively chirped, which is different from the HOS evolution without pre-chirping. We have conducted the HOS evolution in a segment of SMF with or without chirp, and found that the non-chirped and chirped HOS have very similar evolution pictures, except their optimal compression distances are different. Dual-

pulse happens when the pump strength reaches 1400pJ. The position of the minimum width decreases as the pump strength increasing. The soliton order under different pump strengths is shown in Fig. 4(b). We can get from Fig. 4(b) that the soliton order of the pulse at the end of EDF increases with the pump strength increasing, which results in the shorter optical compression distance shown in Fig. 4(a) under higher pump strength because higher order of soliton has shorter optimal compression distance [21–23].

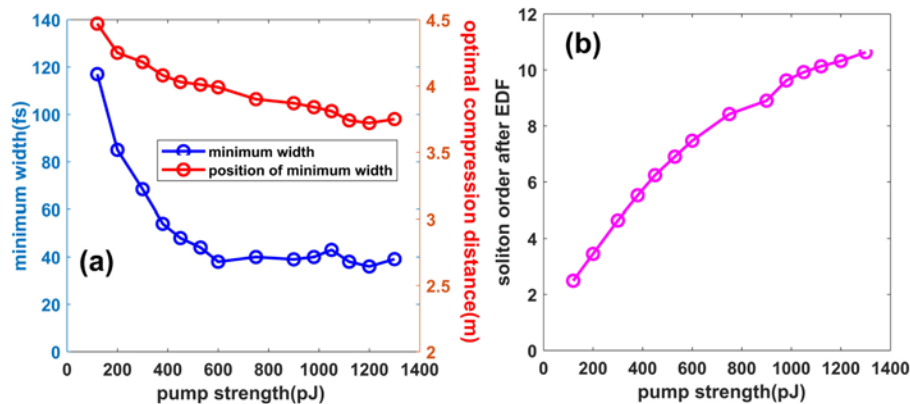


Fig. 4. (a) Minimum width and corresponding position of the stretched-pulse under different pump strengths with zero net-dispersion, (b) soliton order of the pulse at the end of EDF under different pump strengths.

3.3 HOS breaking and recovery

HOS supports ultrashort pulse generation while PBR ensure the HOS exists in the cavity. It is necessary for us to understand why the structured or broken HOS in SMF can be recovered to a smooth pulse in the EDF. It has been proposed in [17] that the broken pulse in the SMF can be recovered to a smooth pulse in EDF in a dispersion-managed GGS fiber laser, which is the same as the case in our paper, however, details of this phenomenon still remain to be researched. Gain, filtering and normal-dispersion are basic characteristics of the EDF. The distortion of the HOS is obviously caused by the nonlinearity, so it is easy for us to know that there must exist a process that compensates the nonlinearity of the broken pulse, which might be the normal-dispersion. Pulse profiles and their corresponding chirps in the case of Fig. 3 are shown in Fig. 5. We can see from Fig. 5(a) that the pulse are strongly nonlinear down chirped at the beginning of the EDF, which is caused by the HOS evolution in the SMF. We should note that due to the nonlinear chirp of the pulse, the pulse components at two or several temporal locations might have the same instantaneous frequency but different phase delays, which result in complicated interference patterns in temporal domain. The distortion or breakage of the pulse can therefore be understood as an interference due to the nonlinear chirp of the pulse. The negative and nonlinear chirp of the pulse will be transformed into a positive and near linear state due to the compensation of the normal-dispersion, which can be seen from Figs. 5(b)-5(d). We can note that there are less nonlinear chirps in the central parts of the pulses in Figs. 5(c) and 5(d), which result in weak interference patterns in temporal domains. The pulse in Fig. 5(d) has a nearly linear chirp across its center while nonlinear chirps still exist at its edges, which results in an almost smooth pulse with slight patterns at edges. The recovery process can be understood as the nonlinear chirp compensation, which decreases the temporal patterns caused by the complicate interference. Gain filtering may also has effects on the recovery of the broken pulse considering the broadband spectra and narrow filtering bandwidth (20nm FWHM of the gain filtering in our model), however, it is not easy for us to analyze this process because the temporal-spectral mapping is complex. We are sure that the normal-dispersion plays an essential role in the recovery of the pulse. We find that the HOS evolution and recovery always

exist in the stretched pulse when the net-dispersion ranges from -0.043ps^2 to 0.024ps^2 . When the net-dispersion is larger than 0.024ps^2 , the pulse tends to behave as a GGS and further increasing the pump strength results in multi-pulsing. When the net-dispersion is smaller than -0.0043ps^2 , the normal-dispersion is not strong enough to compensate the negative and nonlinear chirp of the pulse, and the laser generates unstable pulses when the pump strength is large enough.

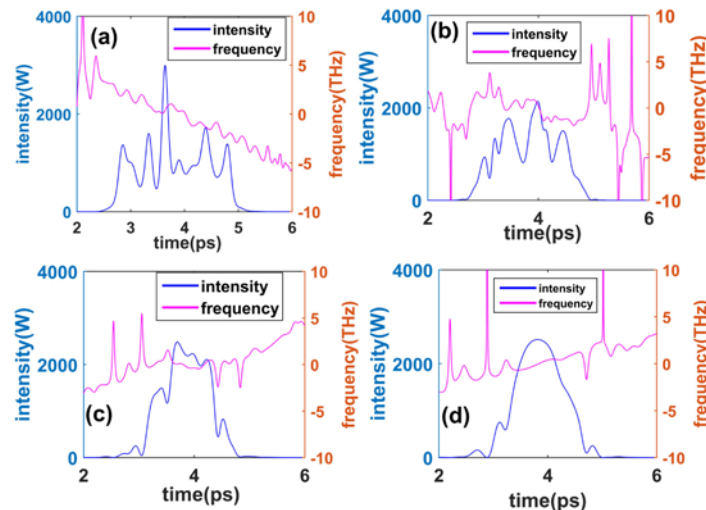


Fig. 5. Pulse characteristics in the case of Fig. 3 at different positions inside the laser: (a) pulse at 0.1m, (b) pulse at 0.4m, (c) pulse at 0.8m, (d) pulse at 1.2m.

4. Discussion

It is necessary to give detailed discussions about the new pulse regime presented in our paper. The HOS evolution in the SMF ensures ultra-narrow temporal width and broadband spectrum generation, however, the accompanying pulse breaking is a natural result of the HOS evolution in the SMF [23]. The pulse breaking during the HOS evolution is caused by the nonlinear chirp induced by the SPM, which results in the complicate temporal interference patterns. The normal dispersion of the EDF can induce linear positive chirp, which can gradually compensate the nonlinear negative chirp accumulated in the SMF. With the nonlinear chirp compensated to the nearly linear positive chirp, the complicate temporal interference patterns of the soliton are also reduced, which results in the smooth pulse profile recovery in the EDF. The normal-dispersion in the EDF should be strong enough to compensate the nonlinear and negative chirp induced by the SPM as well as the anomalous-dispersion in the SMF. We can get from Fig. 4 that the optimal pulse compression position in the cavity can be adjusted by the pump strength, which is similar to the single stage soliton compress in [25], we think in experiments with an OC placed at certain position in the SMF and adjusting the pump strength, one can get the optimal compressed pulse with ultra-narrow width and broadband spectrum from the OC. However, the above thinking needs to be further researched in the experiments.

We think the pulse regime in our proposed laser system can be regarded as the dispersion-managed solitons. Although the pulse evolution in our paper is different from the traditional stretched or dispersion-managed solitons at near-zero net-dispersion, the basic and important method to support the new pulse regime is still the dispersion-management, i.e. the anomalous dispersion supports the HOS evolution while the normal dispersion supports the PBR. Though our proposed new pulse regime can generate high energy pulse with ultra-narrow pulse width, the laser will output multi-pulse if the pulse energy is too strong as one can see from Fig. 6. We can get from Fig. 6 that the dual-pulse state happens under the pump strength of 1400 pJ with

near-zero net-dispersion. The energy of the dual-pulse is ~ 3.1 nJ, which is slightly larger than the 2.9 nJ single pulse energy under the pump strength of 1300pJ. So we think there is a pulse energy limitation for the new pulse regime, beyond which the gain saturation of high energy pulse as well as the gain competition between the high energy pulse and background noise results in the formation of the dual-pulse, such a process can be seen clearly in Fig. 6.

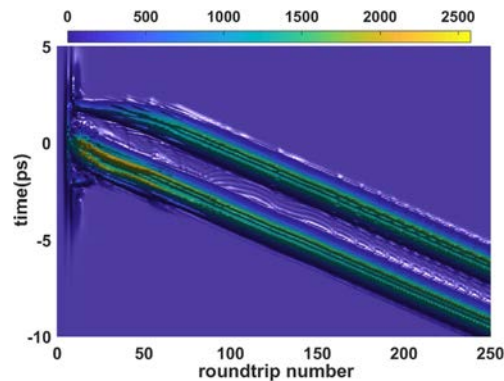


Fig. 6. Round-to-round evolution of the stretched pulse with 1400pJ pump strength, 70% modulation depth and near-zero net-dispersion.

5. Conclusion

In conclusion, we have presented a new regime of the stretched-pulse fiber laser, which combines the HOS evolution and pulse breaking recovery. Transform-limited pulse with ultra-broadband spectrum can be generated due to the HOS evolution while its breaking behavior in the SMF can be compensated by the EDF with normal-dispersion. The pulse breaking recovery can be regarded as the compensation of the nonlinear chirps by the normal-dispersion, which reduces the interference patterns in temporal domain and makes the pulse smooth. Our proposed stretched laser can be used to directly generate non-chirped ultrashort pulse without external compression, which is useful in optical sampling, optical frequency comb and optical fiber communications. Our results can also give insights into the stretched pulse dynamics.

Funding

National Natural Science Foundation of China (NSFC) (61775074); National 1000 Young Talents Program, China; 111 Project (No. B07038).